A Self-Decoupled Circularly Polarized Microstrip Antenna via Cross-Handed Current Cancellation

Zexian Chen, *Graduate Student Member, IEEE*, and Jiangwei Sui, *Member, IEEE*

***Abstract*—This letter presents a compact circularly polarized (CP) microstrip patch antenna (MPA) array with inherent self-decoupling capability for the BeiDou-B3 (1.268 GHz ± 10 MHz) navigation band. Leveraging characteristic mode analysis (CMA), the driven antenna excites co-handed CP currents, whereas the cross-handed CP currents are arranged to cancel out on the coupled antenna, thereby eliminating the need for additional decoupling structures. Simulation and experimental results confirm that the proposed CP MPA array achieves a 20 dB isolation bandwidth of 1.25 GHz to 1.278 GHz (2.22%) while maintaining excellent circular polarization performance. Besides, the proposed self-decoupling technique is demonstrated to be scalable to a 1 × 4 configuration, showcasing its potential for robust anti-jamming systems in the BeiDou-B3 band.**

***Index Terms*—Characteristic mode analysis (CMA), circularly polarized (CP), microstrip patch antenna (MPA), mutual coupling, satellite navigation, self-decoupling.**

I. Introduction

COMPACT multiantenna arrays are widely employed to enhance the anti-jamming capability of navigation systems. However, the dense arrangement of antenna elements often leads to significant mutual coupling effects, which negatively impact system's interference suppression capability and positioning accuracy [1], [2]. On the other hand, circularly polarized (CP) antenna arrays are of great importance in modern satellite navigation systems due to their inherent advantages in multipath mitigation and tolerance to polarization mismatches [3], [4], [5]. Among various antenna types realizing CP radiation, microstrip patch antennas (MPAs) are particularly attractive because they offer advantages such as low profile, light weight, and ease of integration.

To address the severe mutual coupling issue in microstrip antenna arrays, numerous decoupling techniques have been proposed in recent years. The first approach involves introducing additional decoupling elements or structures. A common strategy is to employ band-stop configurations, such as defected ground structures (DGS) [6], [7] and electromagnetic bandgap (EBG) structures [8], [9], [10]. Another method is to introduce cancellation paths to neutralize coupled currents or waves, which is often achieved using parasitic elements [11], [12], [13], decoupling networks [14], [15], or array-antenna decoupling surfaces (ADS) [16], [17]. The second approach leverages the inherent electromagnetic properties of the antenna itself to achieve self-decoupling. This is typically realized by exploiting weak-field regions [18], [19], [20], performing characteristic mode analysis (CMA) [21], [22], [23], [24], or utilizing common-mode and differential-mode cancellation mechanisms [25], [26]. These methods effectively suppress mutual coupling without requiring additional external components, offering a more compact and integrated solution.

However, most existing decoupling techniques are primarily designed for linearly polarized (LP) antenna arrays, which are not suitable for the stringent requirements of satellite navigation systems. While some effective decoupling methods for circularly polarized microstrip patch antenna arrays have been proposed in [7], [13], and [14], these approaches typically rely on additional decoupling structures, which may increase design complexity and reduce integration efficiency. Very recently, a self-decoupling method for CP antenna arrays was introduced in [20], which mitigates the mutual coupling by generating a null-field region, inherently simplifying the design while maintaining the overall performance of the array.

In this letter, a self-decoupled CP MPA array is proposed for the anti-jamming systems in the BeiDou-B3 band. Unlike the approach presented in [20], where a null-field region is used to reduce coupling, the proposed design employs a different strategy: the driven antenna combines co-handed CP currents to enhance radiation performance, while the coupled antenna experiences current cancellation due to the presence of cross-handed components. This mechanism inherently achieves self-decoupling, allowing a wider range of feed position variation on the coupled antenna and thereby offering greater design flexibility.

II. Working Mechanism

A. Antenna Configuration

As shown in Fig. 1, the proposed 1 × 2 self-decoupled array consists of two CP MPAs with a center-to-center spacing of d. Each patch, rotated by 45° and characterized by a length of L_{p} and width of W_{p}, is implemented on a substrate with a relative permittivity of 3.5, loss tangent of 0.003, and thickness of h. Circular polarization radiation is achieved through asymmetric perturbations introduced at four corners of the patch, satisfying $R_{\mathrm{a}} > R_{\mathrm{b}} > R_{\mathrm{c}} > R_{\mathrm{d}}$. Each antenna is fed by a coaxial probe with a radius of 0.65 mm, positioned at an offset distance d_{f} from the geometric center of the patch to ensure proper impedance matching and optimal excitation of the desired modes.

Received 24 September 2025; accepted 13 October 2025. Date of publication 17 October 2025; date of current version 8 January 2026. This work was supported in part by the National Natural Science Foundation of China under Grant 62201625; in part by Guangdong Basic and Applied Basic Research Foundation under Grant 2025A1515010696; and in part by the Science, Technology and Innovation Commission of Shenzhen Municipality under Grant KJZD20240903101314019. *(Corresponding author: Jiangwei Sui.)*

The authors are with the School of Electronics and Communication Engineering, Sun Yat-sen University—Shenzhen Campus, Shenzhen 518107, China (e-mail: chenzx59@mail2.sysu.edu.cn; suijw@mail.sysu.edu.cn).

Digital Object Identifier 10.1109/LAWP.2025.3622651

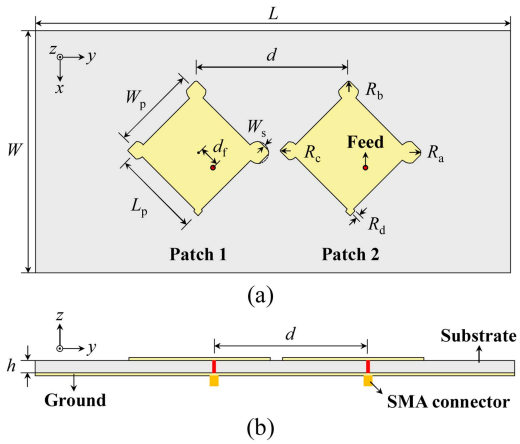

Fig. 1. Structure of the proposed self-decoupled 1 × 2 CP MPA array. (a) Top view. (b) Side view. Dimensions in mm: $L = 285$, $W = 145$, $h = 7$, $d = 91.5$, $W_p = 52$, $L_p = 50.5$, $d_f = 13.5$, $R_a = 6.6$, $R_{b1} = 5.9$, $R_{b2} = 6$, $R_{c1} = 5.3$, $R_{c2} = 5.5$, $R_{d1} = 2.7$, $R_{d2} = 3$, and $W_s = 1.1$.

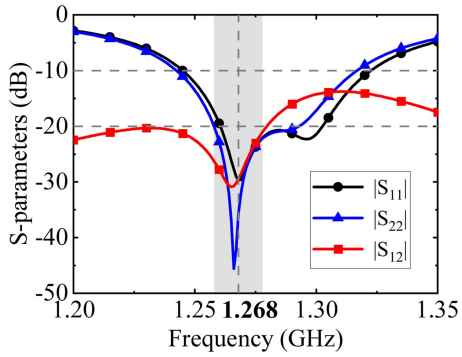

Fig. 2. Simulated *S*-parameters of the proposed 1 × 2 CP MPA array.

B. Decoupling Mechanism

According to the CMA theory [27], the excitability of the *n*th mode depends on its modal significance (MS), defined as

$$MS_n = \left| \frac{1}{1 + j\lambda_n} \right|. \tag{1}$$

MS close to 1 indicates that the mode is easily excited at the given frequency. On the other hand, the characteristic angle (CA) is used to describe the phase difference between the characteristic current and its tangential electric field on the conductor surface, which is given by

$$\alpha_n = 180^\circ - \tan^{-1}\lambda_n. \tag{2}$$

To achieve high-quality CP radiation, it is essential that the two modes possess comparable MS and a 90° CA difference.

The simulated *S*-parameters are presented in Fig. 2, demonstrating that the proposed CP MPA array achieves a high isolation of around 30 dB at 1.268 GHz. To explore the underlying mechanism, a comprehensive CMA study is conducted. As shown in Fig. 3, the CP MPA array shows a CA difference of approximately 90° between the horizontal and vertical modes. Additionally, Modes 1 and 2 have comparable modal significance. As observed from Fig. 3(c), Modes 1 and 2 are the two orthogonal modes primarily responsible for generating CP

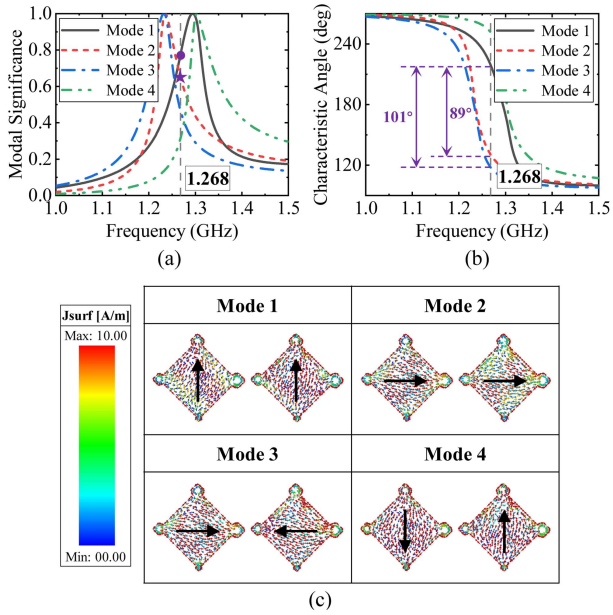

Fig. 3. CMA results of the proposed CP MPA array. (a) Modal significance. (b) Characteristic angle. (c) Four dominant characteristic currents at 1.268 GHz.

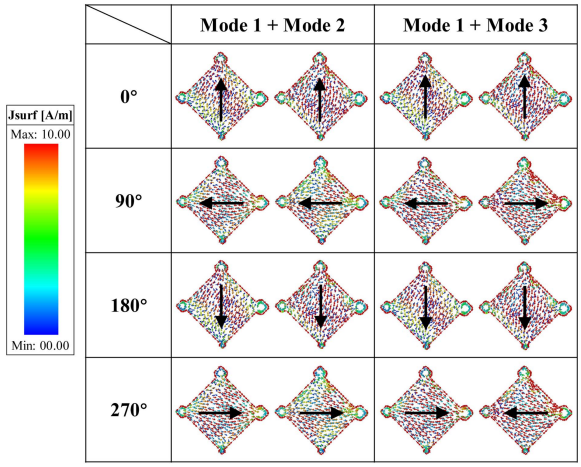

Fig. 4. Modal combination results of the proposed CP MPA array over one period at 1.268 GHz.

radiation, whereas Modes 3 and 4 arise due to the near-field coupling between the patches.

Based on the modal analysis of the proposed array, the characteristic currents of Modes 1 and 2, as well as Mode 1 and Mode 3, are combined, as shown in Fig. 4. When Mode 1 and Mode 2 are superimposed, both the left and right patches exhibit right-handed circular polarization (RHCP). In contrast, the superposition of Modes 1 and 3 results in opposite polarization senses on the two patches: RHCP on the left patch and left-handed circular polarization (LHCP) on the right one. A similar phenomenon is also observed for the Modes 2 and 4 combination, and the results are omitted here for brevity.

To ensure that the driven antenna generates the desired RHCP radiation, the feed position is important. The selection of feed position is mainly guided by the CP characteristics of a single antenna element. It is well known that placing the feed along the central axis of the patch enables effective excitation of CP

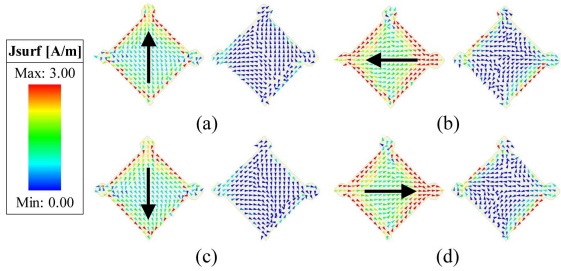

Fig. 5. Simulated current distributions of the proposed CP MPA array at 1.268 GHz. (a) 0°. (b) 90°. (c) 180°. (d) 270°.

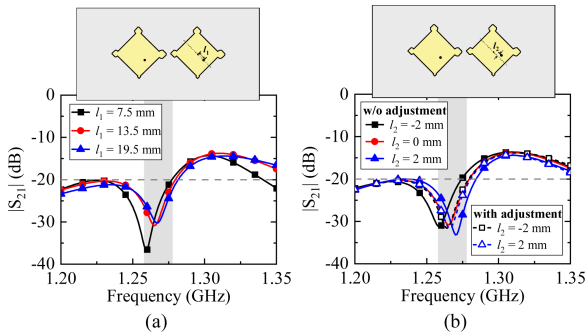

Fig. 6. Effect of the coupled antenna's feeding position on $|S_{21}|$. (a) Effect of l_1 on $|S_{21}|$. (b) Effect of l_2 on $|S_{21}|$.

TABLE I
EFFECT OF R_a ON CHARACTERISTIC MODES

R_a (mm)	Frequency of $MS_1 = MS_2$ (GHz)	$\|CA_1 - CA_2\|$	$\|CA_1 - CA_3\|$	Frequency of min. $\|S_{21}\|$ (GHz)
5.6	1.278	67.6°	84.5°	1.281
6.1	1.27	77.5°	109.8°	1.273
6.6	1.263	90.5°	104.2°	1.265
7.1	1.258	102.2°	113.6°	1.256
7.6	1.25	111.6°	121.8°	1.247

radiation when asymmetric perturbations are introduced to the patch [28]. Then the proposed array is constructed from the single-element antenna. To preserve CP radiation while ensuring self-decoupling performance, the array design primarily relies on CMA to fine-tune the antenna geometry, as illustrated in the following discussion.

As shown in Fig. 5, when patch 1 is excited, the driven antenna exhibits RHCP radiation, while almost no current is induced on the coupled antenna. Therefore, even when the feed point of the coupled antenna is adjusted, it is expected that the array is still able to maintain self-decoupling. However, changing the feed position will affect the excitation strength and phase relationships of different modes, which in turn leads to a slight frequency shift in $|S_{21}|$. Nevertheless, this frequency deviation can be corrected by fine-tuning the antenna dimensions, as shown in Fig. 6(b).

Based on the above analysis, it can be concluded that achieving both CP radiation and self-decoupling in the proposed array critically depends on ensuring that $|CA_1 - CA_2|$ and $|CA_1 - CA_3|$ are both close to 90°. The rotation angle of the patches and the four asymmetric corners serve as important parameters for tuning these phase differences. Taking R_a as an example, as shown in Table I, with the increase of R_a, the frequency of $MS_1 = MS_2$ gradually decreases, while both $|CA_1 - CA_2|$ and $|CA_1 - CA_3|$ also decrease. When $R_a = 6.6$ mm, these two values are both close to 90° and the array achieves favorable CP radiation and self-decoupling performance, as demonstrated in Fig. 7.

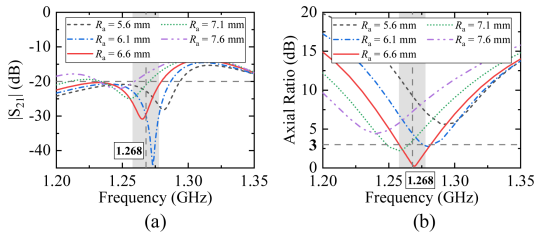

Fig. 7. Effect of R_a on (a) $|S_{21}|$ and (b) axial ratio.

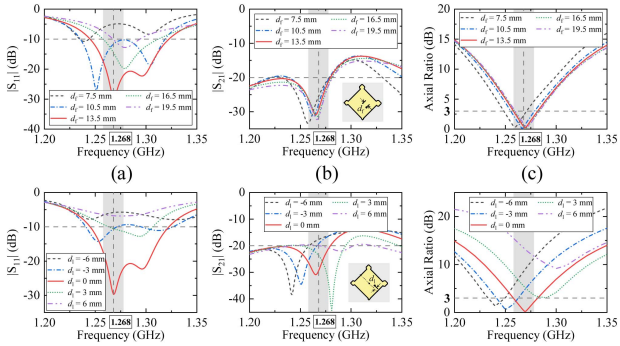

Fig. 8. Effects of feed position on S-parameters and axial ratio of the proposed 1×2 CP antenna array. Effects of d_f on (a) $|S_{11}|$, (b) $|S_{21}|$, and (c) axial ratio. Effects of d_1 on (d) $|S_{11}|$, (e) $|S_{21}|$, and (f) axial ratio.

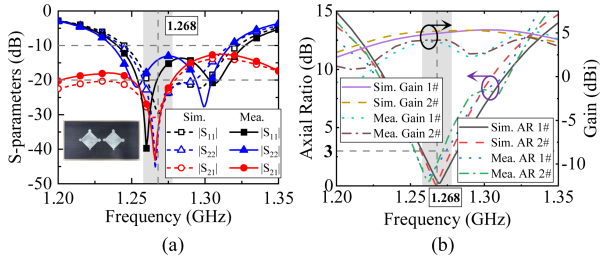

Fig. 9. Simulated and measured results of the proposed CP MPA array. (a) S-parameters. (b) Axial ratio and gain.

To further validate the rationality of the feed points, a two-dimensional sweep of the feed position was performed along both the central axis and the perpendicular direction, as shown in Fig. 8. The results indicate that d_f mainly affects the impedance matching with only a minor impact on the axial ratio (AR), whereas d_1 exerts a pronounced influence on both impedance and AR. This confirms that the feed position has a substantial effect on the excitation strength and phase relationships of the target modes, thereby influencing both the isolation and CP performance of the array.

III. PERFORMANCE EVALUATION AND ANALYSIS

A. Two-Element Antennas

A prototype of the proposed self-decoupled two-element CP antennas is fabricated and measured, as inserted in Fig. 9(a). As shown in Fig. 9, the array achieves a −10 dB impedance bandwidth of 1.24 GHz to 1.317 GHz (6.03%) and maintains an

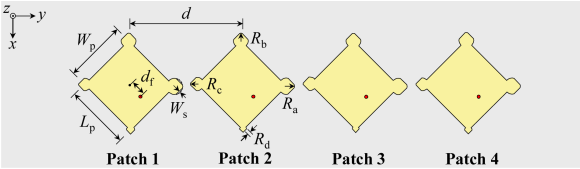

Fig. 11. Structure of the proposed 1 × 4 CP MPA array.

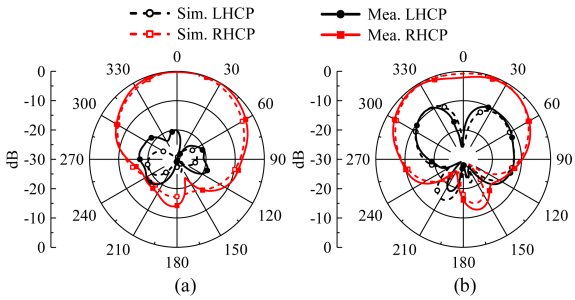

Fig. 10. Simulated and measured normalized radiation patterns of the proposed CP MPA array at 1.268 GHz. (a) Patch 1 at *xz*-plane. (b) Patch 1 at *yz*-plane.

TABLE II
PARAMETER VALUES OF THE 1 × 4 CP MPA ARRAY (UNIT: MM)

Parameter	d	W_{p1}	L_{p1}	d_{f1}	R_{a1}	R_{b1}	R_{c1}
Value	92	52.9	50.5	13.3	6.6	6	5.1
Parameter	R_{d1}	W_{s1}	W_{p2}	L_{p2}	d_{f2}	R_{a2}	R_{b2}
Value	3.4	1.1	52.8	50.1	13.5	6.7	6
Parameter	R_{c2}	R_{d2}	W_{s2}	W_{p3}	L_{p3}	d_{f3}	R_{a3}
Value	5.6	2.8	1.12	52.7	50	13.5	6.7
Parameter	R_{b3}	R_{c3}	R_{d3}	W_{s3}	W_{p4}	L_{p4}	d_{f4}
Value	6	5.6	2.8	1.05	53	50.8	13.3
Parameter	R_{a4}	R_{b4}	R_{c4}	R_{d4}	W_{s4}		
Value	6.6	6	5.1	3.3	1.15		

isolation level better than 20 dB from 1.25 GHz to 1.278 GHz, effectively covering the BeiDou-B3 band. Fig. 9(b) shows that a 3 dB AR bandwidth of approximately 20 MHz is also maintained within 1.252 GHz to 1.272 GHz (1.58%). Within the BeiDou-B3 band, the simulated average gains of Patch 1 and Patch 2 are 4.95 dBi and 5.20 dBi, while the measured average gains are 3.83 dBi and 4.15 dBi, which can be attributed to fabrication tolerances and non-ideal measurement conditions.

Fig. 10 presents the normalized radiation patterns of the proposed array at 1.268 GHz. In both the *xz*- and *yz*-planes, the copolarized (RHCP) radiation patterns of two antennas exhibit high symmetry, further indicating effective self-decoupling performance.

B. 1 × 4 Antenna Array

In this section, the proposed two-element system is readily extended to a 1 × 4 CP MPA array, as shown in Fig. 11, with detailed dimensions listed in Table II.

As the results shown in Fig. 12, the array achieves a −10 dB impedance bandwidth from 1.238 GHz to 1.3 GHz and a 3 dB AR bandwidth of 1.259 GHz to 1.277 GHz. Within the operating frequency range of 1.268 GHz ± 10 MHz, the isolation between any two adjacent antennas exceeds 20 dB, indicating excellent intrinsic decoupling. Additionally, the maximum gains of the edge elements and interior elements are 5.81 dBi and 5.18 dBi, respectively, and the lower gains of the interior elements are

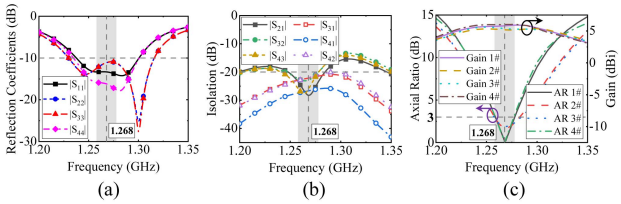

Fig. 12. Simulated performance of the proposed 1 × 4 CP MPA array. (a) Reflection coefficients. (b) Isolation. (c) Axial ratio and gain.

TABLE III
COMPARISON OF THE PROPOSED DESIGN AND RECENT CP MPA ARRAYS

Ref.	Decoupling method	Self-decoupling	Feed	CS	PAA	BW (%)	Gain (dBi)
[7]	DGS	No	Dual	0.36 λ_0	Co-pol.	1.58	4.74
[13]	Parasitic structure	No	Single	0.18 λ_0	X-pol.	0.97	4.7
[14]	Decoupling network	No	Dual	0.42 λ_0	Co-pol.	4.43	NA
[20]	E-fields Counteraction	Yes	Single	0.40 λ_0	Co-pol.	1.79	4.97
[24]	Polarization diversity & shorting pins	Yes	Single	0.20 λ_0	X-pol.	1.25	4.2
Prop.	Cross-Handed Current Cancellation	Yes	Single	0.39 λ_0	Co-pol.	1.58	3.83 /4.15

*CS: Center-to-center spacing. *λ_0: the wavelength at the center frequency in free space. *PAA: Polarization of adjacent antennas. *BW: Overlapping bandwidth of -10 dB impedance, 20 dB isolation, and 3 dB AR bandwidth. *Gain: measured gain at f_0 in the boresight direction ($\theta = 0°$, $\varphi = 0°$).

attributed to the fact that they experience scattering coupling with adjacent elements on both sides. These results demonstrate that the 1 × 4 array not only provides excellent impedance matching and high isolation but also maintains good circular polarization radiation performance.

C. Comparison and Discussion

Table III compares the proposed antenna arrays with existing CP MPA arrays. While all these works can achieve both CP and high isolation, only the designs in [20] and [24], and the proposed arrays utilize self-decoupling techniques, thereby simplifying the overall system design. Besides, the array in [24] supports a compact layout but exhibits narrow bandwidth and opposite polarization between adjacent elements. Compared to the approach in [20], where the feeding position is restricted to a narrow null region to maintain isolation, the proposed design allows the feed point to be adjusted over a wider range without compromising the decoupling performance, thereby offering more design flexibility.

IV. CONCLUSION

A self-decoupling method based on the superposition and cancellation of characteristic currents is proposed for CP MPA arrays. By leveraging the phase information derived from the CMA study, the driven antenna achieves RHCP radiation, while the coupled element experiences the cancellation of cross-handed CP currents, thereby achieving natural high isolation. Both simulated and measured results confirm that the proposed array exhibits effective self-decoupling and robust CP radiation performance. The design features a compact and simple structure, making it a promising candidate for anti-jamming systems in the BeiDou-B3 band.

REFERENCES

[1] Y. Xiong and W. Xie, "Adaptive mutual coupling compensation method for airborne STAP radar with end-fire array," *IEEE Trans. Aerosp. Electron. Syst.*, vol. 58, no. 2, pp. 1283–1298, Apr. 2022.

[2] A. A. Gheethan, P. A. Herzig, and G. Mumcu, "Compact 2 × 2 coupled double loop GPS antenna array loaded with broadside coupled split ring resonators," *IEEE Trans. Antennas Propag.*, vol. 61, no. 6, pp. 3000–3008, Jun. 2013.

[3] Nasimuddin, Y. S. Anjani, and A. Alphones, "A wide-beam circularly polarized asymmetric-microstrip antenna," *IEEE Trans. Antennas Propag.*, vol. 63, no. 8, pp. 3764–3768, Aug. 2015.

[4] F. Tamjid, F. Foroughian, C. M. Thomas, A. Ghahreamani, R. Kazemi, and A. E. Fathy, "Toward high-performance wideband GNSS antennas-design tradeoffs and development of wideband feed network structure," *IEEE Trans. Antennas Propag.*, vol. 68, no. 8, pp. 5796–5806, Aug. 2020.

[5] Nasimuddin, X. Qing, and Z. N. Chen, "A compact circularly polarized slotted patch antenna for GNSS applications," *IEEE Trans. Antennas Propag.*, vol. 62, no. 12, pp. 6506–6509, Dec. 2014.

[6] K. Wei, J.-Y. Li, L. Wang, Z.-J. Xing, and R. Xu, "Mutual coupling reduction by novel fractal defected ground structure bandgap filter," *IEEE Trans. Antennas Propag.*, vol. 64, no. 10, pp. 4328–4335, Oct. 2016.

[7] D. Gao, Z.-X. Cao, S.-D. Fu, X. Quan, and P. Chen, "A novel slot-array defected ground structure for decoupling microstrip antenna array," *IEEE Trans. Antennas Propag.*, vol. 68, no. 10, pp. 7027–7038, Oct. 2020.

[8] F. Yang and Y. Rahmat-Samii, "Microstrip antennas integrated with electromagnetic band-gap (EBG) structures: A low mutual coupling design for array applications," *IEEE Trans. Antennas Propag.*, vol. 51, no. 10, pp. 2936–2946, Oct. 2003.

[9] G. Zhai, Z. N. Chen, and X. Qing, "Enhanced isolation of a closely spaced four-element MIMO antenna system using metamaterial mushroom," *IEEE Trans. Antennas Propag.*, vol. 63, no. 8, pp. 3362–3370, Aug. 2015.

[10] X. Yang, Y. Liu, Y.-X. Xu, and S.-x. Gong, "Isolation enhancement in patch antenna array with fractal UC-EBG structure and cross slot," *IEEE Antennas Wireless Propag. Lett.*, vol. 16, pp. 2175–2178, 2017.

[11] Z. Chen, M.-C. Tang, M. Li, D. Yi, D. Mu, and R. W. Ziolkowski, "Wideband, high-density circularly polarized array with reduced mutual coupling and enhanced realized gain," *IEEE Trans. Antennas Propag.*, vol. 70, no. 2, pp. 1132–1143, Feb. 2022.

[12] T. Pei, L. Zhu, J. Wang, and W. Wu, "A low-profile decoupling structure for mutual coupling suppression in MIMO patch antenna," *IEEE Trans. Antennas Propag.*, vol. 69, no. 10, pp. 6145–6153, Oct. 2021.

[13] K. Wei and B.-C. Zhu, "The novel W parasitic strip for the circularly polarized microstrip antennas design and the mutual coupling reduction between them," *IEEE Trans. Antennas Propag.*, vol. 67, no. 2, pp. 804–813, Feb. 2019.

[14] Z. Wang and Q. Wu, "A novel decoupling feeding network for circularly polarized patch arrays using orthogonal mode decomposition," *IEEE Trans. Antennas Propag.*, vol. 71, no. 2, pp. 1448–1457, Feb. 2023.

[15] Y.-M. Zhang, S. Zhang, J.-L. Li, and G. F. Pedersen, "A transmission-line-based decoupling method for MIMO antenna arrays," *IEEE Trans. Antennas Propag.*, vol. 67, no. 5, pp. 3117–3131, May 2019.

[16] K.-L. Wu, C. Wei, X. Mei, and Z.-Y. Zhang, "Array-antenna decoupling surface," *IEEE Trans. Antennas Propag.*, vol. 65, no. 12, pp. 6728–6738, Dec. 2017.

[17] M. Li, Y. He, C. Zhou, Y. Zhang, and D. Wu, "Design of decoupling and pattern shaping surface for MIMO antennas using the multiport optimization method," *IEEE Trans. Antennas Propag.*, vol. 73, no. 5, pp. 2927–2939, May 2025.

[18] H. Lin, Q. Chen, Y. Ji, X. Yang, J. Wang, and L. Ge, "Weak-field-based self-decoupling patch antennas," *IEEE Trans. Antennas Propag.*, vol. 68, no. 6, pp. 4208–4217, Jun. 2020.

[19] L. Zha, Y. M. Pan, and S. Y. Zheng, "Self-decoupled linear and planar MIMO microstrip patch antenna arrays operating in the fundamental TM_{01} mode," *IEEE Trans. Antennas Propag.*, vol. 72, no. 2, pp. 1224–1233, Feb. 2024.

[20] Q. X. Lai, Y. M. Pan, and S. Y. Zheng, "Mode-counteraction based self-decoupling in circularly polarized MIMO microstrip patch array," *IEEE Trans. Antennas Propag.*, vol. 70, no. 10, pp. 9337–9346, Oct. 2022.

[21] N.-W. Liu, B.-B. Huang, L. Zhu, and G. Fu, "Isolation and bandwidth improvements of multimode single MPA with copolarized pattern using characteristic modes analysis," *IEEE Antennas Wireless Propag. Lett.*, vol. 22, no. 6, pp. 1356–1360, Jun. 2023.

[22] Y. Wang, Q. Xue, and H. Xie, "Wideband decoupled asynchronously coupled patch antennas," *IEEE Trans. Antennas Propag.*, vol. 73, no. 2, pp. 906–919, Feb. 2025.

[23] Q. X. Lai, Y. M. Pan, and S. Y. Zheng, "A self-decoupling method for MIMO antenna array using characteristic mode of ground plane," *IEEE Trans. Antennas Propag.*, vol. 71, no. 3, pp. 2126–2135, Mar. 2023.

[24] N.-W. Liu, L. Zhu, Z.-X. Liu, M. Li, G. Fu, and Y. Liu, "A novel low-profile circularly polarized diversity patch antenna with extremely small spacing, reduced size, and low mutual coupling," *IEEE Trans. Antennas Propag.*, vol. 70, no. 1, pp. 135–144, Jan. 2022.

[25] L. Sun, Y. Li, Z. Zhang, and H. Wang, "Antenna decoupling by common and differential modes cancellation," *IEEE Trans. Antennas Propag.*, vol. 69, no. 2, pp. 672–682, Feb. 2021.

[26] W. Zhang, Y. Li, K. Wei, and Z. Zhang, "A two-port microstrip antenna with high isolation for Wi-Fi 6 and Wi-Fi 6E applications," *IEEE Trans. Antennas Propag.*, vol. 70, no. 7, pp. 5227–5234, Jul. 2022.

[27] Y. Chen and C. Wang, *Characteristics Modes Theory and Applications in Antenna Engineering*. Hoboken, NJ, USA: Wiley, 2015.

[28] S. Gao, Q. Luo, and F. Zhu, *Circularly Polarized Antennas*. Hoboken, NJ, USA: Wiley, Nov. 2013.